Article

Hybrid Density Functional Theory Calculations for the Crystal Structure and Electronic Properties of Al^{3+} Doped KDP Crystals

Yang Li [1,2], Zhenshi Li [1,2], Baoan Liu [1,2,*], Xun Sun [1,2,*], Mingxia Xu [1,2], Lisong Zhang [1,2], Xian Zhao [1] and Guodong Lei [1,2]

1   State Key Laboratory of Crystal Materials, Shandong University, Jinan 250100, China;
    201812699@mail.sdu.edu.cn (Y.L.); 202232813@mail.sdu.edu.cn (Z.L.); mxxu@sdu.edu.cn (M.X.);
    zhls@sdu.edu.cn (L.Z.); zhaoxian@sdu.edu.cn (X.Z.); 202212737@mail.sdu.edu.cn (G.L.)
2   Key Laboratory of Functional Crystal Materials and Device, Ministry of Education, Shandong University,
    Jinan 250100, China
*   Correspondence: baliu@sdu.edu.cn (B.L.); sunxun@sdu.edu.cn (X.S.)

Abstract: Intentionally adding select ions such as Al^{3+} could be helpful in controlling the crystal habit of KDP crystal for high yield of optics. The study of how Al^{3+} ions affect crystal quality can provide a basis for selecting an appropriate doping level without negatively affecting the optical properties of crystals. Here, the influence of Al^{3+} ions on the crystal structure and properties of KDP crystals have been investigated by using first-principles calculations. Theoretical calculations show that Al^{3+} ions mainly replace K sites in KDP crystals and could complex with intrinsic V_H^- point defects to form $Al_K^{2+} + 2V_H^-$ cluster defects. The linear absorption spectra indicate that the presence of Al^{3+} ions has minimal impact on the linear absorption of KDP crystals, aligning well with the experimental findings. And Al^{3+} ions could cause a slight shortening of the band gap of KDP crystals. However, these ions could bring significant deformations of O-H bonds. As the concentration of Al^{3+} ions increase, more O-H bonds linking to PO_4 groups are distorted in KDP crystals. As a result, the structural instability could be fast enhanced with increasing the defect concentration. Therefore, high concentrations of Al^{3+} ions could cause the instability of the crystal structure, which finally affects the laser-induced damage resistance of the KDP crystals. This manuscript contributes to a more comprehensive understanding of the physical mechanisms by which different impurity ions affect the optical properties of KDP crystals.

Keywords: KDP; DFT; optical absorption

1. Introduction

Potassium dihydrogen phosphate (KDP, KH_2PO_4) crystals belong to the tetragonal system at room temperature. The point group is D_{2d}-$\overline{4}$2m [1]. KDP crystals have been widely applied in the fields of laser frequency conversion, electro-optic modulation and optical parametric oscillation due to their outstanding nonlinear optical performance [2–4]. A significant application of KDP crystals is in Pockels cells and frequency converters within high power laser facilities for Inertial Confinement Fusion (ICF) [5,6]. However, the actual laser-induced damage threshold of perfect KDP crystal is at least an order of magnitude lower than the theoretical value, which limits the further development of high power lasers [7–9].

Impurity ions in crystals are considered to be one of the reasons for lowering the laser-induced damage threshold of crystals [10,11]. The effect of different impurity ions on the laser-induced damage property of KDP crystals are different. For example, Fe^{3+} ions and Al^{3+} ions are both common metal impurity ions in growth solution of KDP crystals, but experiments have shown that doping the growth solution with 10 ppm Fe^{3+} leads to a decrease in the laser-induced damage threshold of the crystals, whereas doping with more

than 500 ppm of Al^{3+} only leads to a decrease in the laser-induced damage threshold of the crystals [12–14]. In our previous work, the effect of Fe^{3+} ions on the structure and properties of KDP crystals is investigated using first principles. Fe^{3+} ions introduce impurity states mainly at the band gap of 2.4 eV and 6.6 eV and, at the same time, introduce additional linear absorption at 278 nm, which adversely affects the laser-induced damage threshold of the KDP crystals [15]. After Al^{3+} ions enter the KDP lattice, the point defect centers may be in a non-neutral state as well as possibly charge compensating with intrinsic point defects to form defect clusters. The effect of a small amount of doped aluminum ions on the optical properties of KDP crystals is still unclear. An in-depth analysis of the defects of Al^{3+} ions on the crystal structure, electronic structure and optical properties of KDP crystals can help to understand the effects of different impurity ions on the laser-induced damage threshold of KDP crystals. Moreover, it can provide a reference for choosing the appropriate doping level of Al^{3+} ions regulating the crystal morphology.

In this work, the density functional theory (DFT) is used to study the stability of Al^{3+} ions in KDP crystals, as well as cluster defects consisting of Al^{3+} ions and intrinsic vacancies. The influence of the stabilized defect configuration on the electronic structure, optical properties and crystal structure of KDP crystals is calculated. The physical mechanisms by which Al^{3+} ions affect crystal quality are analyzed.

2. Computational Details and Experimental Methods

2.1. Computational Details

The current calculations are being performed in the Vienna ab initio Simulation Package (VASP) [16,17] utilizing the implementation of density functional theory (DFT) [18–20] along with the projector-augmented-wave (PAW [21,22] formalism. The electron exchange and correlation (XC) functional of the generalized gradient approximation (GGA) [23–26] functional of the Perdew, Burke, Ernzerhof (PBE) [27,28] is used to optimize the configurations. The energetic, electronic and optical properties are employed using the Heyd–Scuseria–Ernzerhof (HSE06) [29–32] hybrid functional system. A kinetic energy cutoff of 680 eV [33–35] is chosen with Monkhorst–Pack *k*-point meshes ($1 \times 1 \times 1$ [15,36,37] for bulk of 256 atoms). The force convergence criterion for the structural relaxation is set to 0.01 eV Å [15,36,38,39]. Thereby the H $1s^1$, P $3s^23p^3$, O $2s^22p^4$, K $4s^1$, Al $3s^23p^1$ states are treated as valence electrons. The lattice constants of unit cell are a = b = 7.50 Å, c = 6.96 Å, and experimental values are a = b = 7.45 Å, c = 6.97 Å [40–42]. The calculated values are in strong agreement with the experimental values.

There are four KH_2PO_4 molecular crystals in a unit cell. We constructed the 256 atoms supercell of KDP crystal containing $2 \times 2 \times 2$ unit cells (along a, b, c axis), and the 3D schematic of this supercell is shown in Figure 1a. The model of Al_K point defect is shown in Figure 1b, where we replaced a K atom at (0.500 0.500 0.750) by a Al atom. In a similar way, we constructed the Al_P and Al_H point defects. In Figure 1c, the Al_P point defect is at (0.500 0.500 0.500). KDP crystals containing one Al_H point defect is shown in Figure 1d, where the Al_H defect is at (0.625 0.570 0.938). The interstitial positions are constructed by adding a Al atom at M_1 (0.250 0.350 0.125) and M_2 (0.750 0.220 0.125) [43], respectively. The defect concentration is 0.39% (1 point defect per 256 atoms system). For the charge state defects, the models are constructed by subtracting or adding an electron to the defect system. For the cluster defects of KDP crystal with Al_K point defect, we built the models by removing the neighboring H atom or K atom. The related structures are also fully relaxed.

In this manuscript, the defect formation energies of point defects with charge state *q* and cluster defects are calculated by this equation [44–46]

$$\begin{aligned} E^f(X^q) = {} & E^{tot}(X^q) - E^{tot}(pristine) \\ & + \sum_i n_i \mu_i + q(E_F + E_v + \Delta V) \end{aligned} \tag{1}$$

where $E^f(X^q)$ is the defect formation energy of the system, $E^{tot}(X^q)$ is the total energy of the defective system and $E^{tot}(pristine)$ is the total energy of the perfect system. n_i, μ_i and

q are the number of atoms removed or added from the supercell, the chemical potential of the defective element and the number of charges carried by the defect, respectively. E_F indicates the position of the Fermi energy level. E_v is the valence-band maximum (VBM) in the pristine KDP. ΔV is the difference of the average electrostatic potential between the defect system and the pristine KDP. KDP crystals are directly grown from aqueous solutions with high purity raw materials by changing temperature in accordance with the solubility curve [47], so we calculated the chemical potentials of Al, K and P using their most stable existence phases at ambient temperature and atmospheric pressure. The chemical potential of H is calculated by taking half of the energy of H_2, and the chemical potentials of K, P and Al are calculated according to the formation enthalpies of their stable compounds K_2O with $Fm\bar{3}m$, Al_2O_3 with $R\bar{3}C$ and P_2O_5 with Fdd_2:

$$2\Delta\mu_K + \Delta\mu_O = -\Delta H_f^{K_2O} \tag{2}$$

$$2\Delta\mu_{Al} + 3\Delta\mu_o = -\Delta H_f^{Al_2O_3} \tag{3}$$

$$2\Delta\mu_P + 5\Delta\mu_O = -\Delta H_f^{P_2O_5} \tag{4}$$

The thermodynamic transition level $\varepsilon(q_1/q_2)$ is defined as the Fermi-level position for which the formation energies of charge states q_1 and q_2 are equal [48,49]

$$\varepsilon(q_1/q_2) = \frac{E_f(X^{q_1}) - E_f(X^{q_2})}{q_2 - q_1} \tag{5}$$

$E_f(X^q)$, q_1 and q_2 indicate the formation energy of the charged system and the number of charges carried by the defect. When the Fermi energy level is below $\varepsilon(q_1/q_2)$, the q_1 state is stable, and conversely, the q_2 state is stable when the Fermi level is above $\varepsilon(q_1/q_2)$.
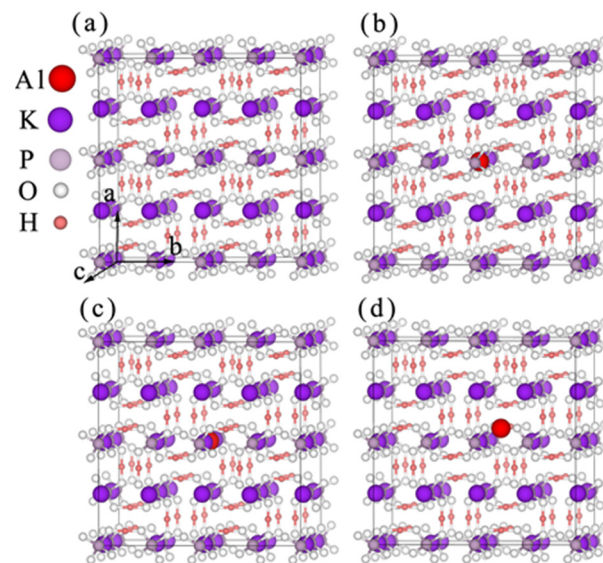

Figure 1. Schematic of KDP crystal supercells. (**a**) KDP crystal supercell; (**b**) KDP crystal containing Al_K point defect; (**c**) KDP crystal containing Al_P point defect; (**d**) KDP crystal containing Al_H point defect.

2.2. Experimental Methods

The point seed rapid growth technique is used to grow KDP crystals. The growth solution for the KDP crystals are prepared as an aqueous solution with a saturation point of 55.0 °C using high purity potassium dihydrogen phosphate powder from Sinopharm Chemical Reagent Co (Shanghai, China). Al^{3+} doped KDP crystals are made by doping 10 ppm $AlCl_3$ to the overheated solution. The grown crystals are processed as $15 \times 15 \times 10$ mm^3 samples. The photograph of KDP samples is given in Figure 2. The transmittance spec-

trum of these samples is obtained by PerkinElmer UV/VIS/NIR Spectrometer Lambda 1050+ (USA).
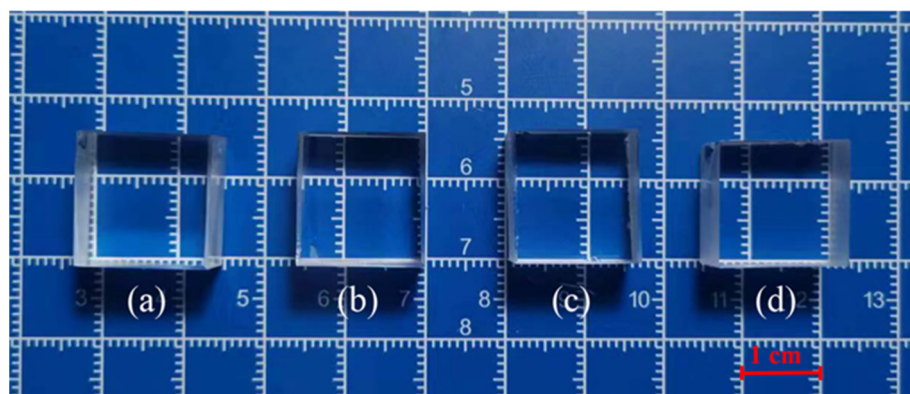

Figure 2. Photograph of KDP samples. (**a**) undoped-prismatic, (**b**) undoped-pyramidal, (**c**) Al^{3+} doped-prismatic, (**d**) Al^{3+} doped-pyramidal.

3. Results and Discussion

3.1. Preferable Substitution Sites and Doping Stability of Al^{3+} Ions in KDP Crystals

Due to the limitation of experimental techniques, no specific characterization of Al^{3+} ions in KDP crystals has been reported in the literature experimentally. So the sites occupied by Al^{3+} ions in the crystals need to be clarified first to build the defect model. Al^{3+} in the growth solution is a trivalent cation and may occupy the sites of three elements H, P, or K. All of these sites need to be considered. In addition, theoretical studies suggest that the metal cations may be in two interstitial positions (M_1 (0.250 0.350 0.125) or M_2 (0.750 0.220 0.125)) in KDP crystals [43]. The state of existence of defects in crystals is related to the thermodynamic properties that can determine the relative stability of defects in crystals. The defect formation energies of these five defect systems are calculated separately, and the concentration of point defects in all of these systems is 0.39%, as shown in Table 1.

Table 1. Formation energy of five different sites in KDP crystal.

Location	Defect Formation Energy (eV)
H (0.625 0.570 0.938)	18.2
P (0.500 0.500 0.500)	9.7
K (0.500 0.500 0.750)	3.3
M_1 (0.250 0.350 0.125)	4.8
M_2 (0.750 0.220 0.125)	5.1

Both H and P sites have high defect formation energies of 18.2 eV and 9.7 eV, respectively. This means Al^{3+} are not thermodynamically easy to substitute H or P sites in KDP crystals. The defect formation energy is relatively low at the K site (3.3 eV) and the two interstitial sites (M_1 4.8 eV, M_2 5.1 eV). Therefore, the priority sties of Al^{3+} in KDP crystals is K > M_1 > M_2, which is thermodynamically most stable when occupying the K site. Accurate calculation of the energies and transition conditions of defects in crystals at different charge states is of great importance for the identification of defects and the subsequent study of neutral defect pairs. In order to research the stability of Al^{3+} substituted K sites point defects (Al_K) at different charge states for further investigation of their composite effect with intrinsic point defects, the defect formation energies of the defect system at different charge states were calculated by Equation (1), where the defect formation energy of a charged defect is a function of the Fermi energy level. And the thermodynamic transition level between deferent charged defects is calculated by Equation (5). Figure 3 shows the defect formation energy and the energy conditions for the charge state transition of Al_K

defects with different charge states in KDP crystals. As the Fermi energy level approaches the VBM, the Al_K point defect center is stabilized as a positive divalent. As the Fermi energy level moves upward to a position of about 4.1 eV, the point defect captures an electron and is stabilized as Al_K^+. As the Fermi energy level continues to move closer to the CBM (at 5.2 eV), the point defect continues to capture a charge, stabilizing as a neutral state. At low defect concentrations, the Fermi energy level of KDP crystals is located at the center of the band gap (3.6 eV), so the Al_K defects are usually stabilized in the form of positive divalent (Al_K^{2+}) in KDP crystals with low concentrations of defects.
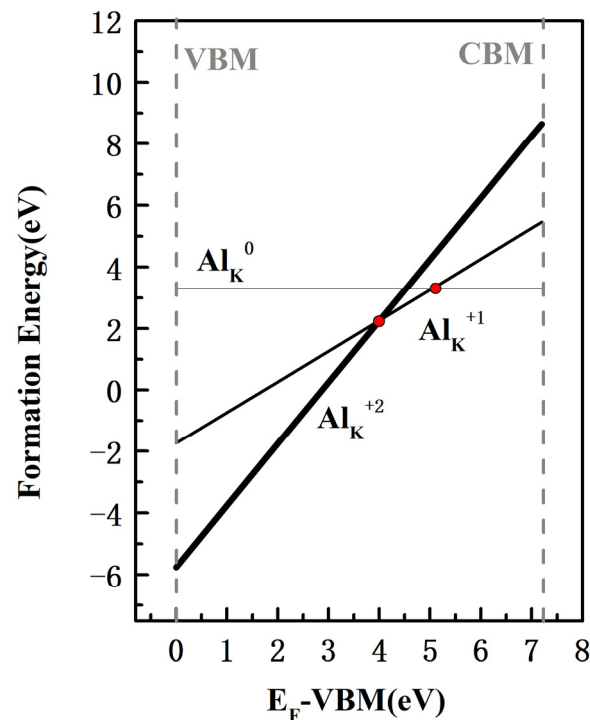

Figure 3. The formation energies of Al_K with different charge states.

According to the defect formation energy calculations, Al^{3+} is thermodynamically most stable in the crystal as Al_K^{2+} point defect. According to the principle of charge compensation, the crystal system is electrically neutral, and theoretically Al_K^{2+} point defect needs to be charge compensated with defects that have a negative charge state. Hydrogen vacancies and potassium vacancies are defect centers with negative charge states in KDP crystal, and it is possible for these defects with negative charge states to charge compensate with Al_K^{2+} to form cluster defects. A positive divalent charge state of Al_K^{2+} needs to be charge-compensated with two potassium vacancies (V_K^-), or two hydrogen vacancies (V_H^-), or one V_K^- and one V_H^-, to form $Al_K^{2+} + 2V_K^-$, $Al_K^{2+} + 2V_H^-$, or $Al_K^{2+} + V_K^- + V_H^-$ defective clusters to keep the system electrically neutral. According to the theoretical study on cluster defects in KDP crystals, the distance between isolated point defects in the cluster defects affects the stability of the cluster defects in the crystals [15,36]. As the distance between isolated point defects decreases, the potential and lattice relaxation energies of the system decrease, so the defect formation energies of the defect clusters decreases and the stability of the defect clusters increases. In building the model for the complexation of Al_K^{2+} with intrinsic point defects, only the stability of the complexation with the nearest neighboring hydrogen vacancies or potassium vacancies is considered. Remove the two K atoms nearest neighbors of Al_K^{2+} (forming the $Al_K^{2+} + 2V_K^-$ cluster defect), the two H atoms (forming the $Al_K^{2+} + 2V_H^-$ cluster defect), and the nearest neighbors of one H atom and one K atom (forming the $Al_K^{2+} + V_K^- + V_H^-$ cluster defect), respectively. Table 2 is the formation energies of the cluster defects models and the coordinates of the point defect in cluster defects models.

Among them, the defect formation energy of the cluster defect $Al_K^{2+} + 2V_H^-$ is 4.1 eV, which is the lowest defect formation energy among these three defect cluster configurations. Therefore, the cluster defect formed by the Al_K^{2+} point defect with two intrinsic V_H^- point defects is thermodynamically the most stable.

Table 2. The formation energies of different cluster defects.

Cluster Defects	Locations	Defect Formation Energy (eV)
$Al_K^{2+} + 2V_K^-$	Al (0.500 0.500 0.750) K_1 (0.500 0.750 0.875) K_2 (0.500 0.250 0.875)	8.7
$Al_K^{2+} + V_K^- + V_H^-$	Al (0.500 0.500 0.750) K (0.500 0.750 0.875) H (0.625 0.570 0.438)	6.8
$Al_K^{2+} + 2V_H^-$	Al (0.500 0.500 0.750) H_1 (0.625 0.570 0.438) H_2 (0.570 0.375 0.563)	4.1

In the energy calculations mentioned in this manuscript, we use the total energy of the system. To accurately calculate the defect formation energies at room temperature, the free energy (when the entropy of the system is small enough, the total energy of the system can be approximated by looking at the free energy of the system) of the system should be used. Because of the large forbidden band, KDP crystals can be seen as insulators, so the value of the electron entropy in the crystal is negligible. But configuration of the constructed $Al_K^{2+} + 2V_H^-$ defect is large, so the conformational entropy may not be negligible. According to the Boltzmann equation, the conformational entropies of the cluster defects have been calculated. The conformational entropies of the $Al_K^{2+} + 2V_H^-$ cluster defect is 10.73×10^{-4} eV/K. Even at room temperature, the conformational entropies of the three defect clusters are still very small. For the system we have calculated, the total energy of the system can be approximated as the free energy of the system. Our use of the total energy of the system for defect stability does not affect our results.

3.2. Properties of Al^{3+} Ions Doping in KDP Crystal

In order to clarify the effect of Al^{3+} on the electronic structure of KDP crystals, the partial density of states (PDOS) of KDP crystals in different defect systems is calculated, as shown in Figure 4. Figure 5 is the charge distribution of KDP crystals containing an Al_K point defect (in Figure 5a) and a cluster defect (in Figure 5b), where the red, white, gray, purple and orange balls are used to represent the H, O, P, K and Al atoms. Blue and yellow regions represent electron depletion and accumulation, respectively. The band gap of the pristine KDP crystal is 7.2 eV. The valance band maximum (VBM) is composed of O 2p states and the conduction band minimum (CBM) is mainly composed of O 2p, K 4s, P 3p and H 1s hybridized electronic states. For the Al_K^{2+} point defect, the CBM of KDP crystals is down to 6.1 eV. The Al_K^{2+} point defect introduces a deep energy defect state in the band gap of the KDP crystals, which is mainly contributed by the Al 3p states, O 2p states and P 3p states. The electric transfer of the Al_K^{2+} point defect is mainly with phosphorus-oxygen tetrahedra in crystals. The charge distribution in Figure 5a can confirm the transfer of electrons. After the charge compensation with two neighboring V_H^- to form the $Al_K^{2+} + 2V_H^-$ cluster defect, the CBM is slightly shifted upward to 6.2 eV, mainly contributed by O 2p states and Al 3p states. From Figure 5b, the charge transfer between Al_K^{2+} and V_H^- attenuates the charge state interaction between Al_K^{2+} and neighboring oxygen atoms. In total, the effect of Al^{3+} on the electronic structure of KDP crystals is mainly seen in causing a downward shift in the crystal CBM, which just has little effect on the crystal electronic structure.
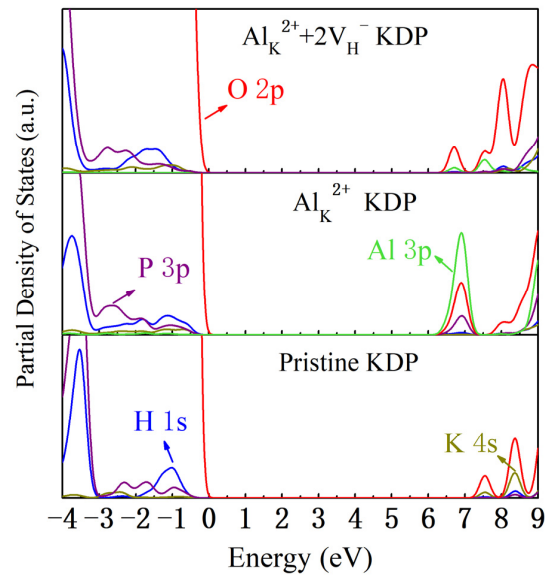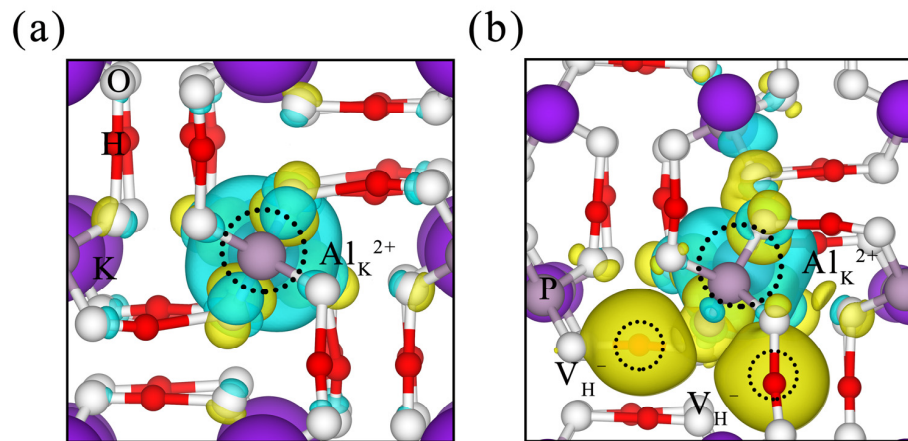
Figure 4. PDOS of KDP crystals.

(a)   (b)

Figure 5. Electronic charge differences of KDP crystal. (**a**) Al_K^{2+} KDP, (**b**) $Al_K^{2+} + 2V_H^-$ KDP.

To clarify the optical properties of the KDP crystals containing Al^{3+} ions, the optical properties of pristine KDP crystals, KDP crystals containing Al_K^{2+} point defects and KDP crystals containing $Al_K^{2+} + 2V_H^-$ cluster defects, which are mainly determined by the dielectric function, are calculated separately. The dielectric function $\varepsilon(\omega)$ is used to describe the linear response of a material to an electromagnetic radiation [50]

$$\varepsilon(\omega) = \varepsilon_1(\omega) + i\varepsilon_2(\omega) \tag{6}$$

The $\varepsilon_2(\omega)$ is the frequency-dependent imaginary part of the dielectric function [50,51]

$$\varepsilon_2(\omega) = \frac{c}{\omega^2} \sum_{V,C} \int_{BZ} \frac{2}{(2\pi)^2} |M_{C.V}(k)|^2 \cdot \delta\left(E_C^k - E_V^k - \hbar\omega\right) d^3k \tag{7}$$

The $\varepsilon_1(\omega)$ is the real part of the dielectric function, which is obtained by the Kramers–Kronig relations [50,51]

$$\varepsilon_1(\omega) = 1 + \frac{2}{\pi} p \int_0^\infty \frac{\varepsilon_2(\omega')\omega'd\omega'}{(\omega'^2 - \omega^2)} \tag{8}$$

The absorption coefficient further obtained from the dielectric function [52]

$$I(\omega) = \sqrt{2}(\omega)\left(\sqrt{\varepsilon_1(\omega)^2 + \varepsilon_2(\omega)^2} - \varepsilon_1(\omega)\right)^{\frac{1}{2}} \tag{9}$$

The absorption $I(\omega)$ of KDP crystals is shown in Figure 6. Compared with the pristine KDP crystals, there are no additional absorption peaks induced by Al_K^{2+} point defects or $Al_K^{2+} + 2V_H^-$ cluster defects in the wavelength range of 200 nm to 800 nm. The effect of Al^{3+} ions on the light absorption of KDP crystals is mainly reflected in the introduction of weak light absorption at 160–190 nm. It is close to the theoretical absorption cut-off edge of KDP crystals, and difficult to be observed in experimental tests. UV-Vis spectrophotometry showed that Al^{3+} ions have no significant effect on the transmittance of the KDP crystals [12]. The calculated light absorption of the defects in the crystals is in agreement with the experimental results. The reason for the insignificant effect on the crystal light absorption is that the effect of Al^{3+} ions on the electronic structure of the crystal mainly causes a decrease in the CBM, and the crystal remains in a wide band gap, where valence electrons are still difficult to generate leaps.
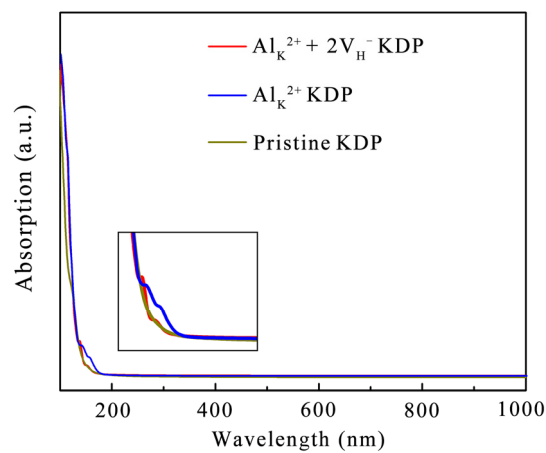

Figure 6. Linear optical absorption of KDP crystals.

A transmission measurement has been implemented for the undoped and Al^{3+} doped KDP crystals. The transmission spectra of these samples are shown in Figure 7. It can be seen that there is no significant difference in the ultraviolet region through these spectra. This is consistent with the theoretical calculation results. Therefore, low concentration Al^{3+} ions can be doped during crystal growth to control crystal morphology without seriously reducing crystal optical quality.
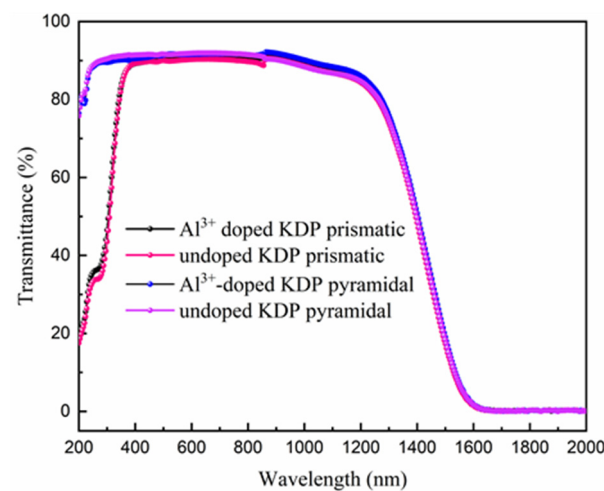

Figure 7. Transmission spectra of undoped and Al^{3+} doped KDP crystals.

The analysis of electronic and optical properties shows that Al^{3+} ions have a minor effect on KDP crystals. The alteration of electronic structure and optical absorption may not

be the main mechanism by which Al^{3+} ions lead to the lowering of the laser-induced damage threshold of KDP crystals. Based on experimental observations, at high concentrations (>50 ppm), Al^{3+} ions cause cracking in the crystals. The effect of Al^{3+} ions on the crystal structure of KDP crystals cannot be ignored. To study the effect of Al^{3+} ions on the crystal structure of KDP crystals, the variations in O-H and P-O bonds are calculated as follows

$$\Delta = \left| \frac{D(defect\ state) - D(pristine\ system)}{D(pristine\ system)} \right| \tag{10}$$

where D (*defect state*) and D (*pristine system*) are the bond lengths for the chemical bonds in the defective and pristine systems, respectively. The results are shown in Figure 8, where the horizontal axis is the distance apart from the defects center (0 Å represents the bond nearest to defect center), and the vertical coordinate is the variation in different chemical bonds. At the defect center, Al_K^{2+} point defects and $Al_K^{2+} + 2V_H^-$ cluster defects induce 39.3% and 33.2% variations in O-H bonds, respectively. The variations come from the electrostatic interactions between the Al_K^{2+} defects and the neighboring oxygen atoms. These interactions weaken the electrostatic attraction between the neighboring oxygen atoms and the hydrogen atoms connected to them, giving a certain degree of repulsion to the H atoms, which results in the displacement of the H atoms. The variations in O-H bonds induce 3.2% (Al_K^{2+} point defects) and 1.3% ($Al_K^{2+} + 2V_H^-$ cluster defects) variations in P-O bonds connected to them. Al^{3+} ions induce minor effects on the P-O bonds, however, induce larger variations in the O-H bonds connecting phosphorus-oxygen tetrahedra in KDP crystals. The overall trend of the aberrations of the O-H bonds is decreasing with relaxation in the crystal cell. However, at 8 Å, the variations in the O-H bond in both Al_K^{2+} point defects and $Al_K^{2+} + 2V_H^-$ cluster defects systems are still greater than 10%. When the concentration of Al^{3+} ions in the crystal is higher, the concentration of Al_K^{2+} and $Al_K^{2+} + 2V_H^-$ defects in the crystal is higher. It will lead to more variations in O-H bonds connected to the phosphorus-oxygen tetrahedral skeleton in the KDP crystals, and the structural stability of the crystals will be damaged. Through the analysis of the defect system structure, the high concentration of Al^{3+} ions will lead to the destabilization of the KDP crystal structure, which will ultimately affect the optical properties of the KDP crystals.
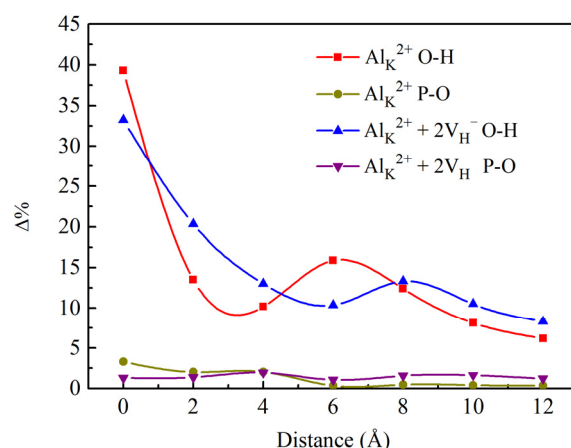

Figure 8. The variations in O-H and P-O bonds as a function of the distance apart from the defects.

4. Conclusions

The effects of Al^{3+} ions on the electronic structure, optical absorption and crystal structure of KDP crystals are investigated by DFT, and the mechanism of the influence of Al^{3+} ions on the laser-induced damage threshold of the crystals is analyzed. Through the stability analysis of different defect systems, Al^{3+} ions mainly occupy K sites in the KDP crystals, forming Al_K^{2+} point defects. Al_K^{2+} easily compensates with the intrinsic hydrogen vacancies in the crystal through charge compensation, forming $Al_K^{2+} + 2V_H^-$ cluster defects. Based on the analysis of the electronic structure and optical properties of the

doped KDP crystals, the Al^{3+} ions only lead to a downshift in the crystal CBM that is not sufficient to cause significant defect-assisted multiphoton absorption. This weak change in the electronic structure makes the position of the linear absorption peak induced by Al^{3+} ions very close to the theoretical cut-off absorption edge of the KDP crystals. The effect of Al^{3+} ions on the linear absorption of KDP crystals is also small. However, by analyzing the structure of the doped KDP crystals, it is found that the Al^{3+} ions induce large variations in the O-H bonds. When the concentration of Al^{3+} ions in the crystal is high, the variations in the O-H bonds connecting the phosphorus-oxygen tetrahedral skeleton accumulates with the increase in ions concentration. The structural stability of the crystal is damaged, which in turn affects the optical properties of the crystal, and the laser-induced damage threshold of the crystal decreases. In conclusion, at low concentrations, Al^{3+} ions have little effect on the laser-induced damage threshold of KDP crystals, while at high concentrations, the stability of the crystal structure is destroyed, leading to a decrease in the laser-induced damage threshold of the crystals. This suggests that choosing the appropriate level of Al^{3+} ions doping does not negatively affect the optical properties of KDP crystals.

Author Contributions: Conceptualization, Y.L. and B.L.; methodology, M.X. and L.Z.; software, X.Z.; validation, Y.L. and Z.L.; formal analysis, Y.L. and Z.L.; investigation, G.L.; resources, X.S.; data curation, Y.L.; writing—original draft preparation, Y.L.; writing—review and editing, B.L. and X.S.; supervision, B.L.; project administration, X.S.; funding acquisition, X.S. All authors have read and agreed to the published version of the manuscript.

Data Availability Statement: The original contributions presented in the study are included in the article, further inquiries can be directed to the corresponding author.

Conflicts of Interest: The authors declare no conflicts of interest.

References

1. Rashkovich, L.N.; Shlakhova, O. *KDP-Family Single Crystals*; CRC Press: Boca Raton, FL, USA, 2021.
2. Nikogosyan, D.N. *Nonlinear Optical Crystals: A Complete Survey*; Springer Science & Business Media: New York, NY, USA, 2006.
3. Han, W.; Xiang, Y.; Li, F.; Wang, F.; Zhou, L.; Zhao, J.; Feng, B.; Zheng, K.; Zhu, Q.; Wei, X. Evaluating the safe limit of large-aperture potassium dihydrogen phosphate crystals associated with transverse stimulated Raman scattering. *Appl. Opt.* **2015**, *54*, 4167–4171. [CrossRef]
4. Guzman, L.A.; Suzuki, M.; Fujimoto, Y.; Fujioka, K. Habit control of deuterated potassium dihydrogen phosphate crystal for laser applications. *J. Phys. Conf. Ser.* **2016**, *688*, 012024. [CrossRef]
5. Hawley-Fedder, R.; Geraghty, P.; Locke, S.; Mcburney, M.; Runkel, M.; Suratwala, T.; Thompson, S.; Wegner, P.; Whitman, P. NIF Pockels cell and frequency conversion crystals. In *Optical Engineering at the Lawrence Livermore National Laboratory II: The National Ignition Facility*; SPIE: Bellingham, DC, USA, 2004; Volume 5341.
6. De Yoreo, J.J.; Burnham, A.K.; Whitman, P.K. Developing KH_2PO_4 and KD_2PO_4 crystals for the world's most power laser. *Int. Mater. Rev.* **2002**, *47*, 113–152. [CrossRef]
7. Stuart, B.C.; Feit, M.D.; Herman, S.; Rubenchik, A.M.; Shore, B.W.; Perry, M.D. Nanosecond-to-femtosecond laser-induced breakdown in dielectrics. *Phys. Rev. B* **1996**, *53*, 1749. [CrossRef] [PubMed]
8. Carr, C.W.; Radousky, H.B.; Rubenchik, A.M.; Feit, M.D.; Demos, S.G. Localized dynamics during laser-induced damage in optical materials. *Phys. Rev. Lett.* **2004**, *92*, 87401. [CrossRef] [PubMed]
9. Campbell, J.H.; Hawley-Fedder, R.A.; Stolz, C.J.; Menapace, J.A.; Borden, M.R.; Whitman, P.K.; Yu, J.; Runkel, M.J.; Riley, M.O.; Feit, M.D. NIF optical materials and fabrication technologies: An overview. In *Optical Engineering at the Lawrence Livermore National Laboratory II: The National Ignition Facility*; SPIE: Bellingham, DC, USA, 2004; Volume 5341, pp. 84–101.
10. Hopper, R.W.; Uhlmann, D.R. Mechanism of inclusion damage in laser glass. *J. Appl. Phys.* **1970**, *41*, 4023–4037. [CrossRef]
11. Feit, M.D.; Rubenchik, A.M. Implications of nanoabsorber initiators for damage probability curves, pulselength scaling, and laser conditioning. In *Laser-Induced Damage in Optical Materials: 2003*; SPIE: Bellingham, DC, USA, 2004.
12. Lu, Y.Q.; Wang, S.L.; Mu, X.M.; Ding, J.X.; Sun, Y.; Wang, Z.P.; Cheng, X.F.; Xu, X.G.; Wang, B. Effect of Al^{3+} impurity on the optical properties of KDP crystal. *J. Funct. Mater.* **2010**, *5*, 915–917.
13. Lu, Y.Q.; Wang, S.L.; Xu, X.G.; Sun, X.; Gu, Q.T.; Mu, X.M.; Liu, B. Effects of Al^{3+} Ion on the Growth Habit of KDP Crystals. *Bull. Chin. Ceram. Soc.* **2009**, *4*, 631–635.
14. Sun, X.; Zhang, Y.Z.; Xu, M.X.; Sun, S.T.; Ji, L.L.; Wang, Z.P.; Li, K.Y.; Cheng, X.F.; Xu, X.G. Effect of Fe^{3+} Ion on the Optical Properties of KDP Crystal. *J. Synth. Cryst.* **2007**, *36*, 1240–1244.

15. Li, Y.; Liu, B.; Li, Y.; Sui, T.; Zhao, X.; Xu, M.; Sun, X. Hybrid density functional theory calculations for the electronic and optical properties of Fe^{3+}-doped KDP crystals. *CrystEngComm* **2022**, *24*, 8082–8088. [CrossRef]

16. Becke, A.D. Density-functional exchange-energy approximation with correct asymptotic behavior. *Phys. Rev. A* **1988**, *38*, 3098. [CrossRef]

17. Kresse, G.; Furthmüller, J. Efficiency of ab-initio total energy calculations for metals and semiconductors using a plane-wave basis set. *Comp. Mater. Sci.* **1996**, *6*, 15–50. [CrossRef]

18. Yang, W.T. Direct calculation of electron density in density-functional theory. *Phys. Rev. Lett.* **1991**, *66*, 1438. [CrossRef] [PubMed]

19. Kohn, W.; Sham, L.J. Self-Consistent equations including exchange and correlation effects. *Phys. Rev.* **1965**, *140*, A1133. [CrossRef]

20. Kohn, W.; Hohenberg, P. Inhomogeneous electron gas. *Phys. Rev.* **1964**, *136*, B864–B871.

21. Kresse, G.; Joubert, D. From ultrasoft pseudopotentials to the projector augmented-wave method. *Phys. Rev. B* **1999**, *59*, 1758–1775. [CrossRef]

22. Blochl, P.E. Projector augmented-wave method. *Phys. Rev. B Condens. Matter.* **1994**, *50*, 17953–17979. [CrossRef] [PubMed]

23. Grimme, S.; Ehrlich, S.; Goerigk, L. Effect of the damping function in dispersion corrected density functional theory. *J. Comput. Chem.* **2011**, *32*, 1456–1465. [CrossRef]

24. Janesko, B.G.; Barone, V.; Brothers, E.N. Accurate surface chemistry beyond the generalized gradient approximation: Illustrations for graphene adatoms. *J. Chem. Theory Comput.* **2013**, *9*, 4853–4859. [CrossRef]

25. Perdew, J.P.; Burke, K.; Ernzerhof, M. Generalized gradient approximation made simple. *Phys. Rev. Lett.* **1996**, *77*, 3865. [CrossRef]

26. Perdew, J.P.; Wang, Y. Accurate and simple analytic representation of t he electron-gas correlation energy. *Phs. Rev. B* **1992**, *45*, 13244. [CrossRef] [PubMed]

27. Ernzerhof, M.; Scuseria, G.E. Assessment of the Perdew–Burke–Ernzerhof exchange-correlation functional. *J. Chem. Phys.* **1999**, *110*, 5029–5036. [CrossRef]

28. Kresse, G.; Furthmüller, J. Efficient iterative schemes for ab initio total-energy calculations using a plane-wave basis set. *Phys. Rev. B* **1996**, *54*, 11169. [CrossRef] [PubMed]

29. Jiang, X.; Li, Y.; Wei, L.; Xu, M.; Zhang, L.; Chen, J.; Sun, X. First-principles studies on optical absorption of [010] screw dislocation in KDP crystals. *CrystEngComm* **2021**, *23*, 7412–7417. [CrossRef]

30. Heyd, J.; Peralta, J.E.; Scuseria, G.E.; Martin, R.L. Energy band gaps and lattice parameters evaluated with the Heyd-Scuseria-Ernzerhof screened hybrid functional. *J. Chem. Phys.* **2005**, *123*, A1133–A1357. [CrossRef] [PubMed]

31. Krukau, A.V.; Vydrov, O.A.; Izmaylov, A.F.; Scuseria, G.E. Influence of the exchange screening parameter on the performance of screened hybrid functionals. *J. Chem. Phys.* **2006**, *125*, 224106. [CrossRef] [PubMed]

32. Henderson, T.M.; Paier, J.; Scuseria, G.E. Accurate treatment of solids with the HSE screened hybrid. *Phys. Status Solidi (B)* **2011**, *248*, 767–774. [CrossRef]

33. Liu, C.S.; Kioussis, N.; Demos, S.G.; Radousky, H.B. Electron- or hole-assisted reactions of H defects in hydrogen-bonded KDP. *Phys. Rev. Lett.* **2003**, *91*, 15505. [CrossRef]

34. Liu, C.S.; Zhang, Q.; Kioussis, N.; Demos, S.G.; Radousky, H.B. Electronic structure calculations of intrinsic and extrinsic hydrogen point defects in KH_2PO_4. *Phys. Rev. B* **2003**, *68*, 224107. [CrossRef]

35. Liu, C.S.; Hou, C.J.; Kioussis, N.; Demos, S.G.; Radousky, H.B. Electronic structure calculations of an oxygen vacancy inKH_2PO_4. *Phys. Rev. B* **2005**, *72*, 134110. [CrossRef]

36. Li, Y.; Hao, G.; Bai, J.; Sui, T.; Wei, L.; Sun, X.; Zhao, X.; Xu, M.; Liu, B. Structural and electronic properties and optical absorption of oxygen vacancy cluster defects in KDP crystals: Hybrid density functional theory investigation. *CrystEngComm* **2023**, *25*, 2959–2965. [CrossRef]

37. Monkhorst, H.J.; Pack, J.D. Special points for brillouin-zone integrations. *Phys. Rev. B* **1976**, *13*, 5188. [CrossRef]

38. Li, Y.; Jiang, X.; Wu, P.; Zhang, L.; Liu, B.; Li, Y.; Zhao, X.; Sun, X.; Xu, M. Insight into the stability and properties of zn-doped KH_2PO_4 crystal by hybrid density functional theory. *Cryst. Res. Technol.* **2023**, *58*, 2200107. [CrossRef]

39. Sui, T.T.; Wan, C.B.; Xu, M.X.; Sun, X.; Xu, X.G.; Ju, X. Hybrid density functional theory for the stability and electronic properties of Fe-doped cluster defects in KDP crystal. *CrystEngComm* **2021**, *23*, 7839–7845. [CrossRef]

40. Zhang, Q.; Chen, F.; Kioussis, N.; Demos, S.G.; Radousky, H.B. Ab initio study of the electronic and structural properties of the ferroelectric transition in KH_2PO_4. *Phys. Rev. B* **2001**, *65*, 24108. [CrossRef]

41. Hendricks, S.B. The crystal structure of potassium di-hydrogen phosphate. *Am. J. Sci.* **1927**, *s5–s14*, 269–287. [CrossRef]

42. West, J. A quantitative X-ray analysis of the structure of potassium dihydrogen phosphate (KH_2PO_4). *Ferroelectrics* **1987**, *71*, 1–9. [CrossRef]

43. Eremina, T.; Kuznetsova, V.; Eremin, N.; Okhrimenko, T.; Furmanova, N.; Efremova, E.; Rak, M. On the mechanism of impurity influence on growth kinetics and surface morphology of KDP crystals—II: Experimental study of influence of bivalent and trivalent impurity ions on growth kinetics and surface morphology of KDP crystals. *J. Cryst. Growth* **2005**, *273*, 586–593. [CrossRef]

44. Van de Walle, C.G.; Neugebauer, J. First-principles calculations for defects and impurities: Applications to III-nitrides. *J. Appl. Phys.* **2004**, *95*, 3851–3879. [CrossRef]

45. Lany, S.; Zunger, A. Assessment of correction methods for the band-gap problem and for finite-size effects in supercell defect calculations: Case studies for ZnO and GaAs. *Phys. Rev. B Condens. Matter Mater. Phys.* **2008**, *78*, 235104. [CrossRef]

46. Freysoldt, C.; Grabowski, B.; Hickel, T.; Neugebauer, J.; Kresse, G.; Janotti, A.; Van de Walle, C.G. First-principles calculations for point defects in solids. *Rev. Mod. Phys.* **2014**, *86*, 253–305. [CrossRef]

47. Cai, D.; Lian, Y.; Chai, X.; Zhang, L.; Yang, L.; Xu, M. Effect of annealing on nonlinear optical properties of 70% deuterated DKDP crystals at 355 nm. *CrystEngComm* **2018**, *20*, 7357–7363. [CrossRef]

48. He, J.; Behera, R.K.; Finnis, M.W.; Li, X.; Dickey, E.C.; Phillpot, S.R.; Sinnott, S.B. Prediction of high-temperature point defect formation in TiO_2 from combined ab initio and thermodynamic calculations. *Acta Mater.* **2007**, *55*, 4325–4337. [CrossRef]

49. Xu, H.X.; Lee, D.H.; He, J.; Sinnott, S.B.; Phillpot, S.R. Stability of intrinsic defects and defect clusters in $LiNbO_3$ from density functional theory calculations. *Phys. Rev. B* **2008**, *78*, 174103. [CrossRef]

50. Lucarini, V.; Saarinen, J.J.; Peiponen, K.; Vartiainen, E.M. *Kramers-Kronig Relations in Optical Materials Research*; Springer Science & Business Media: Berlin/Heidelberg, Germany, 2005.

51. Xia, Q.L.; Pan, L.X.; Peng, Y.D.; Li, L.Y.; Wang, H.Z.; Bao, R.; Yi, J.H. First principles investigation of electronic structure, chemical bonding, elastic and optical properties of novel rhenium nitrides. *Key Eng. Mater.* **2012**, *512–515*, 883–889. [CrossRef]

52. Chen, X.; Zhao, Q.; Wang, X.; Chen, J.; Ju, X. Linear optical properties of defective KDP with oxygen vacancy: First-principles calculations. *Chin. Phys. B* **2015**, *24*, 77801–77802. [CrossRef]